# Shape optimisation of a two-phase ejector for $CO_2$ refrigeration systems

Michal Palacz[a,*], Jacek Smolka[a], Andrzej J. Nowak[a], Krzysztof Banasiak[b], Armin Hafner[c]

[a]*Institute of Thermal Technology, Silesian University of Technology, Konarskiego 22, 44-100 Gliwice, Poland*
[b]*SINTEF Energy, Kolbjørn Hejes v. 1D, Trondheim, 7465, Norway*
[c]*Department of Energy and Process Engineering, NTNU, Kolbjørn Hejes vei 1d, Trondheim, 7465, Norway*

**Abstract**

The shape optimisation of four $CO_2$ ejectors is presented in this study. The considered ejectors were originally designed for a multi-ejector supermarket $CO_2$ refrigeration system. The objective function was formulated to consider the multiple operating regimes, where the goal of the optimisation was to maximise the device efficiency. Six geometrical parameters were considered in the optimisation procedure. The applied optimisation scheme was a combination of a genetic algorithm coupled with the effective and validated CFD tool, ejectorPL. The optimisation results showed that the ejector efficiency improved by 6%. The shape modification trends were similar for all of the considered ejectors. All of the shape modifications resulted in a smoother expansion inside the motive nozzle, less intense turbulence inside the mixer and a more uniform velocity field inside the mixer. The obtained results showed that the presented methodology can be effectively used for ejector design for numerous applications.

*Keywords:* multi-ejector system, $CO_2$ ejector, ejector optimisation, parallel compression, ejector performance, R744

## Nomenclature

| | |
|---|---|
| $D$ | diameter, m |
| $h$ | specific enthalpy, $J\,kg^{-1}$ |
| $L$ | length, m |
| $\dot{m}$ | mass flow rate, $kg\,s^{-1}$ |
| $OF$ | objective function |
| $p$ | pressure, Pa |
| $s$ | specific entropy, $J\,kg^{-1}\,K^{-1}$ |
| $t$ | temperature, $°C$ |
| $u$ | velocity, $m\,s^{-1}$ |
| $x$ | weighting factor, - |
| $y$ | ejector dimension, mm |

*Greek Symbols*

| | |
|---|---|
| $\chi$ | mass entrainment ratio, - |
| $\eta$ | efficiency, - |
| $\gamma$ | angle, ° |
| $\varphi$ | ratio between base and optimum geometry, - |

*Subscripts*

| | |
|---|---|
| $AVG$ | average |
| $BASE$ | baseline desing |
| $CFD$ | computed value |
| $CON$ | convergent angle |
| $DIF$ | diffuser |
| $DIV$ | divergent angle |
| $EJ$ | ejector |
| $in$ | inlet |
| $MAX$ | maximum |
| $MCH$ | pre-mixing chamber |

---

*Tel.: +48 322372810; fax: +48 322372872
michal.palacz@polsl.pl

| | | | | |
|---|---|---|---|---|
| $MIX$ | mixer | | $out$ | outlet |
| $MN$ | motive nozzle | | $SN$ | suction nozzle |
| $n$ | number of operating conditions | | | |
| $OPT$ | optimum desing | | $UNI$ | uniform |

## 1. Introduction

Due to the number of regulations, such as the Kyoto protocol and the F-gas regulation, the phase-in of low global warming potential (GWP) refrigerants is imminent. However, not only does low-GWP criteria play an important role in the selection of a refrigerant, the properties of the working fluid, such as toxicity, flammability and accessibility, are also considered as major factors when a refrigeration system is chosen by the final customer. The aforementioned characteristics of the refrigerant are extremely important for supermarket refrigeration systems. From the supermarket point of view, the reliability and serviceability of the refrigeration unit are crucial. Fortunately, carbon dioxide can fulfil all of the aforementioned requirements and can be successfully used as the refrigerant. Nevertheless, because of the thermodynamic properties of the fluid, CO2-based refrigeration units generally work in transcritical mode. In consequence, the throttling losses are relatively high. To overcome this drawback, two-phase ejectors are increasingly being installed in such systems.

According to recently published works, application of these ejectors can significantly improve the coefficient of performance (COP) of the refrigeration system, as shown by Elbel and Hrnjak (2008), Nakagawa et al. (2011), Liu et al. (2012a), Banasiak et al. (2012), Lucas and Koehler (2012), Besagni et al. (2016), Elbel and Lawrence (2016) and Haida et al. (2016a). Moreover, Girotto (2012) showed the possibility of improving the COP by 20% even for high ambient temperatures. Similar findings were reported by Lawrence and Elbel (2015). Nevertheless, the cooling capacity control of ejector-based systems is challenging. In literature, two approaches have been used; the first approach uses a multi-ejector block (Hafner et al. (2014); Banasiak et al. (2015)), and second approach uses one controllable ejector (Liu et al. (2012c,a,b); Xu et al. (2012)). Recently, Smolka et al. (2016) analysed the performance of the both approaches showing that in some specific needle positions the multi-ejector unit can outperform the single controllable ejector.

Nevertheless, the aforementioned COP improvements are possible only with a properly designed ejector. Hence, significant effort has been invested in ejector performance analysis. The ejector performance is commonly evaluated by a dimensionless factor, the ejector efficiency ($\eta_{EJ}$), which was introduced by Elbel (2011).

$$\eta_{EJ} = \chi \cdot \frac{h|_{s=s_{SN,in}\,p=p_{DIF,out}} - h_{SN,in}}{h_{MN,in} - h|_{s=s_{MN,in}\,p=p_{DIF,out}}} \tag{1}$$

The ejector efficiency is defined as the ratio of expansion work recovered by the ejector to the maximal potential work rate possible to recover, as described by Eq. (1). To better understand the efficiency definition the state points used in the equation are presented in the $p-h$ diagram (Fig. 1). $\chi$ in the Eq. (1) is called the mass entrainment ratio and it is the ratio between the suction nozzle mass flow rate and the motive nozzle mass flow rate, as described by Eq. (2). These two factors have been used by numerous authors to assess the ejector performance for various operating regimes or different ejector shapes.

$$\chi = \frac{\dot{m}_{SN}}{\dot{m}_{MN}} \tag{2}$$

Recent studies have shown that the relation between the ejector performance and ejector shape is substantial. Nakagawa et al. (2011) experimentally investigated the influence of the mixer length on the ejector performance. Three mixer lengths were considered in the study, 5 mm, 15 mm and 25 mm. The results presented by Nakagawa et al. (2011) showed an extremely strong correlation between the mass entrainment ratio and the mixer length. A complementary investigation was performed by Banasiak et al. (2012)), where various ejector mixer shapes were investigated. Banasiak et al. (2012) tested four mixer diameters ($D_{MIX}$), which ranged from 2 mm to 5 mm, and three optional mixer lengths $5 \times D_{MIX}$, $10 \times D_{MIX}$ and $20 \times D_{MIX}$. In addition, the authors of that investigation analysed the three diffuser divergence angles such as 5°, 7.5° and 10°. That diffuser angles were tested for the
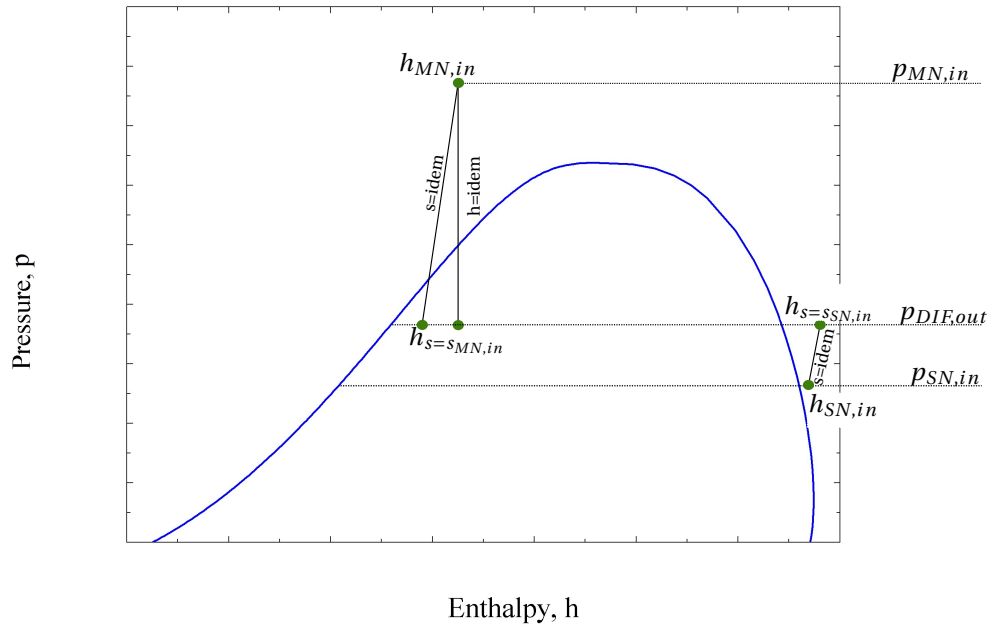
Fig. 1 – Expansion of the primary fluid and compression of the secondary fluid inside a two-phase ejector

$D_{MIX}$ equal to 3 mm. The ejector performance was calculated for all tested geometrical variants. The results of the analysis showed that the mixer diameter had the most significant influence on the ejector efficiency. The change in $D_{MIX}$ from 3 mm to 5 mm decreased $\eta_{EJ}$ by 20%. However, the relation between the ejector efficiency and the diffuser diverging angle was not strong.

To more deeply investigate the influence of the shape of each part of the ejector on $\eta_{EJ}$, Banasiak et al. (2014) performed a numerical investigation of the $CO_2$ ejector performance. To estimate the relation between the ejector shape and its performance, the authors used the relative increased entropy rate inside the ejector. In addition, the efficiency of each ejector section was calculated. The results of the study showed that the motive and suction nozzles are the most efficient parts of the ejector and do not affect the overall performance of the device significantly. On the other hand, the increase in entropy rate was substantial inside the mixer. Moreover, a sensitivity analysis showed that the mixer diameter is the most important geometrical parameter from an ejector performance point of view.

A similar investigation was performed by Sierra-Pallares et al. (2016) for an R134a ejector. Similarly to Banasiak et al. (2014), the rate of entropy increase was analysed. Moreover, Sierra-Pallares et al. (2016) analysed the entropy generation inside the ejector and its effect on the ejector performance. Three different mechanisms of entropy generation were considered, namely the mean viscous dissipation, fluctuating dissipation and heat transfer. The extremely detailed results presented by the authors once again showed that the mixer shape is crucial for the ejector efficiency. Hence, that part of the ejector should be carefully designed. Moreover, as the authors suggested, an efficient mixer design for single operating conditions can be far from optimal for different operating conditions. Therefore, the mixer design procedure should consider additional operating condition characteristics for the considered system.

Taking into account the importance of the ejector mixer shape, Palacz et al. (2016) performed CFD-based shape optimisation of the ejector mixer. To perform the optimisation, two optimisation algorithms were combined with the effective computational tool *ejectorPL*. The ejector efficiency was maximised to increase the ejector performance. Moreover, various operating conditions were considered in the proposed objective function. Two objective functions were considered by Palacz et al. (2016), the first one took into account two sets of operating conditions, and the second one took into account eight sets of operating conditions. The results obtained by

the application of the second objective function showed the improvement of the efficiency for the wider range of operating conditions. Unfortunately, the $\eta_{EJ}$ increase of 2% was not fully satisfying. However, the methodology presented by these authors can be effectively used for ejector shape design.

The approach introduced by Palacz et al. (2016) can be used to design the ejector shape "from scratch" for the considered application. Moreover, the flexibility of the computational tool can be used to perform simulations or optimisation of the device for various working fluids. Therefore, in this study, this computational tool was combined with a genetic algorithm (GA) to perform shape optimisation of four ejectors that were originally designed for a multi-ejector supermarket refrigeration unit. In consequence, all the considered operating regimes were typical for the refrigeration units installed in supermarkets. Thus, the objective of this work is to maximise the performance of the ejectors for such regimes.

To maximise the $\eta_{EJ}$, the six geometrical parameters describing the ejector mixer and the ejector nozzles were selected for the optimisation procedure. Comparing to Palacz et al. (2016), three additional dimensions were considered to investigate the relation between the nozzles and the mixer geometry. Moreover, the suction nozzle operating conditions were different comparing to the one used in previous work of the authors Palacz et al. (2016). Namely, the suction nozzle temperatures used in the objective function were more typical for the food storage. It is also worth mentioning that the way the operating conditions for the objective function were selected in different manner than in the previous work of the authors (see Palacz et al. (2016)). The applied operating conditions were selected to consider not only the ejector operation envelope but also the characteristic of the ejector operation, high pressure lift high mass entrainment ratio. The objective function was formulated to take into account four sets of operating conditions that are typical of a supermarket refrigeration unit. In addition, the optimal ejectors performance was assessed for the test operating conditions to prove that the efficiency improvement can be obtained for a wide range of operating conditions.

The ejector efficiency was improved for all of the considered ejectors and operating conditions. The average efficiency increase was 6%, which is assumed as a significant improvement considering the relatively high efficiencies of the ejectors before optimisation. Moreover, the introduced ejector shape optimisation exhibited similar trends as those mentioned in earlier studies. The mixer diameter was found to be the most important geometrical parameter for the ejector efficiency, where the mixer of the optimal design was significantly longer than in the base design. Nevertheless, the presented results showed that to obtain the high efficiency of the ejectors, the design procedure should include both the mixer and the motive nozzle shape optimisation.

## 2. Ejector design

The general concept of the design of a two-phase ejector is relatively simple. The typical two-phase $CO_2$ ejector is a combination of a few elements, such as the motive nozzle, suction nozzle, mixer and diffuser. A schematic image of this combination is presented below (Fig. 2). In addition, the pre-mixing chamber is presented in the figure. The mixer is an assembly of the converging pre-mixing chamber and the constant cross-section part. The length of the converging part of the mixer is determined by the distance between the motive nozzle outlet and the inlet to the constant cross-section of the mixer (Banasiak et al. (2014); Palacz et al. (2016). The shape of the suction ducts, as presented in Fig. 2, can differ for various ejector designs; see Smolka et al. (2013); Banasiak et al. (2014); Lucas et al. (2014); Nakagawa et al. (2011). However, considering the high isentropic efficiencies of the nozzles, the influence of that part on the ejector efficiency can be omitted. In consequence, the ejector geometry can be reduced to an axisymmetric form. A similar approach was used by Palacz et al. (2016).

Originally, the ejectors considered in this study were designed for a multi-ejector supermarket refrigeration unit. This system is equipped with four ejectors (EJ1-4) that suck the vapour through the suction side and two ejectors (LEJ1-2) that were designed to suck the liquid as the secondary flow. Each ejector installed in the multi-ejector rack was designed to support a different system load. Moreover, parallel ejector operation is possible in such a system. In this way, the cooling capacity of the system is controlled by the 16 ejector operation configurations, as described in Smolka et al. (2016)), who investigated the efficiency of the ejectors in a multi-ejector rack and compared it to the efficiency of a controllable ejector that can be used to control the cooling capacity. The results showed that the multi-ejector unit ejectors can outperform the controllable ejectors. The multi-ejector refrigeration system that was investigated by Haida et al. (2016a) demonstrated that the application of ejectors provided significant COP improvements. Moreover, Haida et al. (2016b) numerically investigated the performance of
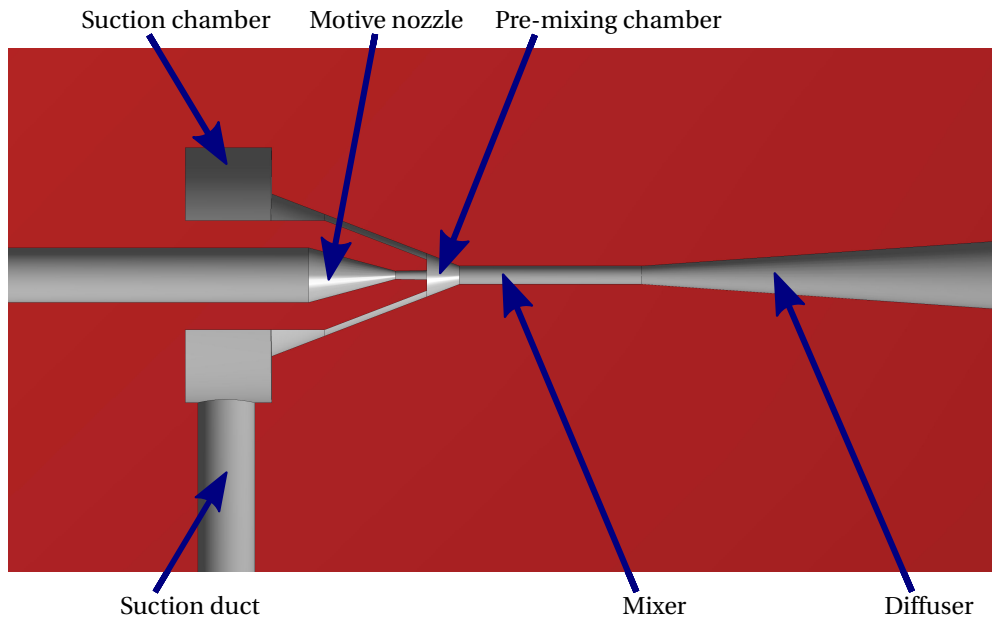
Fig. 2 – Schematic of a two-phase ejector assembly

the liquid ejectors and performed a sensitivity analysis of the ejector shape on the ejector efficiency. However, in this study, only the vapour sucking ejectors were optimised.

The base ejector design was calculated using the 1-D model introduced by Banasiak and Hafner (2011). Then, the ejectors were manufactured and installed in the SINTEF Energy laboratory experimental rig, as described by Haida et al. (2016a). The cooling capacity of this system is rated at 70 kW at a 35°C gas cooler temperature. Finally, the ejectors were manufactured and experimentally investigated. The detailed ejector design and the design procedure are presented in the work of Banasiak et al. (2015), which also presents the experimentally determined efficiencies of these ejectors. The recorded values of $\eta_{EJ}$ exceeded 30% for a broad range of operating conditions. Thus far, the highest $\eta_{EJ}$ reported in the literature (see Sag et al. (2015)) was equal to 40%. Nevertheless that high $\eta_{EJ}$ was recorded for only one operating regime.

To improve the performance of the aforementioned ejectors, an optimisation procedure was applied. The shape optimisation procedure considered the shape optimisation of the mixer shape as well as the motive and suction nozzle shapes. The design of these parts can be described by six geometrical parameters, the mixer length ($L_{MIX}$), mixer diameter ($D_{MIX}$), pre-mixing chamber length ($L_{MCH}$), motive nozzle outlet diameter ($D_{MN}$), motive nozzle diverging angle ($\gamma_{DIV}$) and finally, the suction nozzle converging angle ($\gamma_{CON}$). According to Banasiak et al. (2014), the diffuser shape does not affect the ejector performance as significantly as the mixer shape. Moreover, the shape of the diffuser was designed within the recommendations presented in the work of Banasiak et al. (2012). Hence, the shape of that part was excluded from the optimisation procedure. The simplified axisymmetric ejector geometry as well as the aforementioned geometrical parameters are presented in Fig. 3. The naming convention shown in the figure will be used throughout this paper.

## 3. Optimisation procedure

The optimisation approach was similar to that presented by Palacz et al. (2016). The optimisation algorithm combined with a computational tool was used to perform the optimisation. The applied computational tool was a combination of the commercial packages Ansys FLUENT and Ansys ICEM CFD. The mathematical formulation that was used to perform all of the computations was based on the homogeneous equilibrium model (HEM) approach. A genetic algorithm was used as the optimisation algorithm. The utilised GA was similar to that used by Palacz et al. (2016).
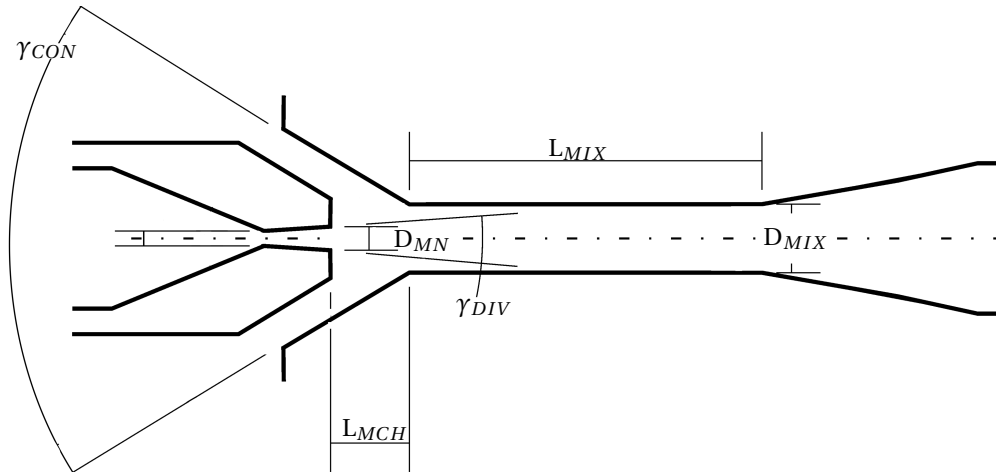
Fig. 3 – Simplified schema of the ejector geometry and the optimised geometrical parameters

### 3.1. Computational tool

The *ejectorPL* computational tool was used to simulate $CO_2$ flow through the ejector. This tool is an in-house developed script that executes the mesh generation procedure and the solving procedure (Palacz et al. (2015, 2016)). The schematic view of the software is presented in Fig. 4. First, the ejector geometry (2-D axisymmetric) and the computational mesh are generated. The meshes were fully structural and were composed of approximately 9000 cells to obtain mesh-independent results. Moreover, the crucial parts of the mesh, e.g., where sonic waves may occur, were refined. In addition, the initialisation procedure was optimised to model the expansion of transcritical fluid inside the device. In this way, the computational time was reduced to 20 minutes per case using two cores of an Intel Xeon processor. Parallel simulations were performed on the Institute of Thermal Technology computational cluster referred to as TOLA; this powerful computing unit consists of 13 computing nodes. Each node is equipped with two Intel Xeon processors (10 physical cores each). Hence, up to 260 cores can be used for parallel computations. The Ansys FLUENT solver that was used was also controlled with the *ejectorPL* script. The mathematical model used for the computation is described in detail by Smolka et al. (2013). In this approach, two-phase flow is modelled within HEM. The NIST REFPROP (Lemmon et al. (2010)) real fluid libraries were implemented in the solver to obtain the refrigerant transport properties. The realisable k-$\epsilon$ model was used to account for turbulence. Pressure boundary conditions were used to close the mathematical description of the model.

The accuracy of the computational tool and mathematical formulation itself was assessed by Palacz et al. (2015). The fidelity of the model was evaluated by comparison of the measured and computed mass flow rates of the motive and suction nozzles. This comparison was performed for over 100 operating regimes. The results of the analysis showed good HEM accuracy for the range of motive nozzle operating conditions, which were close to the $CO_2$ critical point. In addition, the accuracy of the 3-D and 2-D axisymmetric approach was compared by Palacz et al. (2016). The comparison showed good agreement between the 2-D and 3-D models. The 2-D computations tended to underestimate the suction nozzle mass flow rate for all cases. The average errors for the motive nozzle and suction nozzle mass flow rates were 2.6% and 5.2%, respectively.

### 3.2. Optimisation algorithm

A genetic algorithm was used for the shape optimisation of the ejector. The GA applied for the optimisation was previously used by Palacz et al. (2016) to optimise the ejector mixer. Moreover, this code has been used for shape optimisation by a number of authors, such as Munoz et al. (2011); Corriveau et al. (2010); Smolka (2013a,b). The results presented by the aforementioned authors showed that the applied GA can effectively be used for shape optimisation. In addition, the applied optimisation algorithm is easy to customise for a specific problem and couple it with a CFD model.
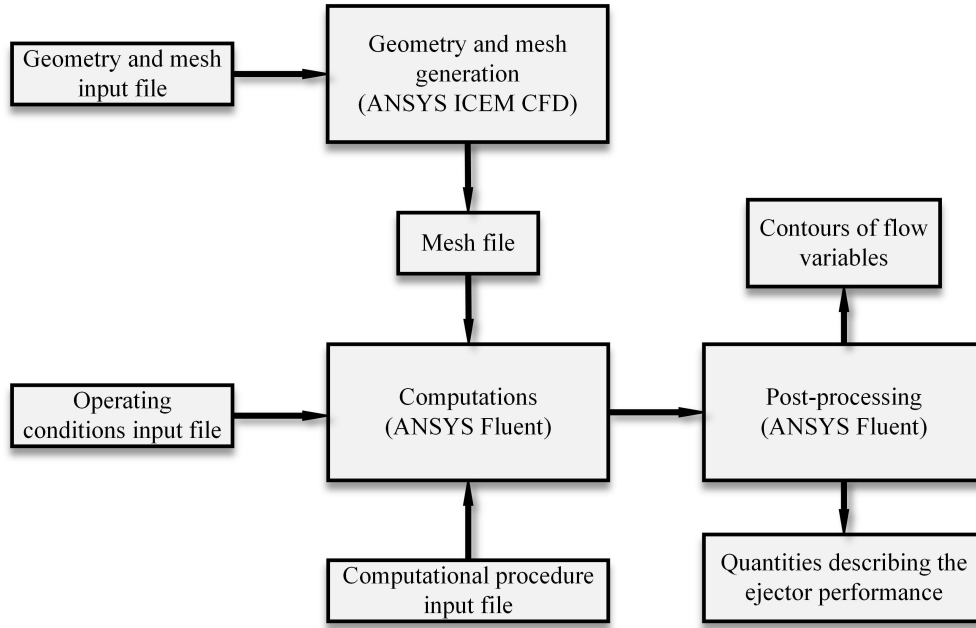
6

Fig. 4 – The flowchart of the *ejectorPL* governing script (Palacz et al. (2015, 2016))

The GA was similar to the one presented by Palacz et al. (2016). The population size was 10 individuals per generation. The uniform crossover between the individuals, jump mutations and creep mutations were performed with a probability equal to 0.5, 0.2 and 0.04, respectively (Corriveau et al. (2010); Smolka (2013a); Palacz et al. (2016)). Moreover, the elitism strategy was used to keep the best individual. The optimal solution was obtained after approximately 40 generations. The GA executes the following steps (Palacz et al. (2016)):

1. The control program executes the GA code, which generates a population of geometrical parameters
2. The population of geometrical parameters is written as input for the computational tool (*ejectorPL*)
3. The control program runs the computations for all generated individuals, where each one is computed for the defined number of operating regimes
4. The Fortran control code checks whether all the computational tool processes are finished
5. The computational tool runs a post-processing procedure for all individuals
6. The GA code processes the computation result files to calculate the objective function (OF)
7. The control code returns to Step 1 to begin the next generation

### 3.3. Objective function

As has already been mentioned, the objective function was defined to maximise the ejector efficiency. Taking into account the ejector efficiency definition (Eq. (1)) and the pressure boundary condition used in the mathematical model, the ejector efficiency can be maximised by the maximisation of $\chi$. Hence, according to Palacz et al. (2016)), the general form of the objective function can be formulated as in Eq.(3).

$$OF_n = \sum_{i=1}^{n} x_n \cdot \chi_n \tag{3}$$

As can be seen, many operating regimes can be used. Moreover, different weighting factors ($x$) can be used in the approach. However, the number of the operating regimes used in the OF affects the computational time significantly. Hence, the objective function used in this study was defined for four ORs (Eq. 4).

$$OF_4 = \sum_{i=1}^{4} 0.25 \cdot \chi_i \tag{4}$$

7

Taking into account the dependency of the optimisation results on the ORs considered in the objective function (see Palacz et al. (2016)), the operating regimes for the OF were carefully selected. The ORs considered for $OF_4$ are listed in Table 1. Moreover, all of the ORs were assumed as the on-design conditions. In consequence, the weighting factor ($x$) is the same for all ORs. The chosen operating regimes represent high pressure ratio conditions and high $\chi$ conditions. The selected ORs are typical motive nozzle operating conditions for supermarkets refrigeration units located in central and southern Europe; see Hafner et al. (2014). The values of the nozzles inlet parameters as well as the outlet parameters for given ORs were captured during the test campaign of the baseline ejectors at SINTEF Energy, Trondheim, Norway. The operating regimes presented in Table 1 were captured during the experimental investigation of the EJ2. The experimental rig used to capture the ejectors inlet and outlet parameters as well as the mass flow rates was described in detail by Banasiak et al. (2015) and Haida et al. (2016a). According to the mentioned studies, the experimental rig was equipped with the Coriolis type mass flow meters, PT1000 calibrated thermocouples and calibrated piezoelectric elements for the mass flow rate, temperature and pressure measurements, respectively. The accuracy of the mentioned sensors was following: $\pm\ 0.5 \times 10^{-3}$ kg·s$^{-1}$ for the mass flow rate measurements, $\pm\ 0.6$ K for the temperature measurements and $\pm\ 2.5\times 10^{4}$ Pa for the pressure measurements. Moreover, the selected operating regimes are distributed close to or above the $CO_2$ critical point.

Table 1 – OF$_4$ operating regimes

|  | Motive nozzle | | Suction nozzle | | Outlet |
|---|---|---|---|---|---|
| ORs | p, bar | t, °C | p, bar | t, °C | p, bar |
| 1 | 72.07 | 26.81 | 29.27 | 3.18 | 38.09 |
| 2 | 75.13 | 28.13 | 27.06 | 1.82 | 34.47 |
| 3 | 96.54 | 37.86 | 26.74 | 0.89 | 37.59 |
| 4 | 98.41 | 38.71 | 25.38 | -2.05 | 34.58 |

Therefore, according to Palacz et al. (2015), the applied mathematical model guarantees accurate results for that set of conditions.

As was previously mentioned, to maximise the ejector performance, six geometrical parameters that describe the nozzles and mixer geometry were selected: mixer length ($L_{MIX}$), mixer diameter ($D_{MN}$), pre-mixing chamber length ($L_{MCH}$), motive nozzle outlet diameter ($D_{MN}$), motive nozzle diverging angle ($\gamma_{DIV}$) and suction nozzle converging angle ($\gamma_{CON}$). A detailed description of the baseline geometry as well as the designing procedure can be found in Banasiak et al. (2015). The variation range for each considered parameter is listed in Table 2. The number of possibilities was 20 for all of the optimised parameters. Considering that the baseline shape of the mixer of the ejector was already close to the optimum (Palacz et al. (2016)) the variation in the dimensions ($D_{MIX}$, $L_{MIX}$, $L_{MCH}$) describing that part was the smallest. However, the relatively high number of possibilities for these parameters helped capture the optimal mixer shape. Moreover, the variation of the motive nozzle diverging angle is extremely small and thus, does not affect the motive nozzle diverging part length too much. As can be seen in Table 2, the range for the converging and diverging angles were the same for all of the considered ejectors.

Table 2 – Variation range of the considered geometrical parameters

|  | $L_{MCH}$, mm | | $L_{MIX}$, mm | | $D_{MIX}$, mm | | $D_{MN}$, mm | | $\gamma_{DIV}$, ° | | $\gamma_{CON}$, ° | |
|---|---|---|---|---|---|---|---|---|---|---|---|---|
|  | Min. | Max. | Min. | Max. | Min. | Max. | Min. | Max. | Min. | Max. | Min. | Max. |
| EJ1 | 1.00 | 4.70 | 7.00 | 35.00 | 1.30 | 4.60 | 1.12 | 1.90 | 1.50 | 3.00 | 20.00 | 50.00 |
| EJ2 | 2.00 | 6.00 | 10.00 | 50.00 | 2.00 | 5.50 | 1.42 | 2.75 | 1.50 | 3.00 | 20.00 | 50.00 |
| EJ3 | 3.70 | 8.00 | 10.00 | 50.00 | 3.00 | 7.50 | 2.00 | 3.00 | 1.50 | 3.00 | 20.00 | 50.00 |
| EJ4 | 4.00 | 10.00 | 20.00 | 70.00 | 5.65 | 10.00 | 2.05 | 3.00 | 1.50 | 3.00 | 20.00 | 50.00 |

## 4. Ejector shape modifications

The numerous modifications of the ejector shape were introduced within the optimisation procedure. To better understand the difference between the reference ejector shape and the optimised shape, all of the geometry

changes will be discussed in this section. The detailed description of the base ejector shape was presented in recent works of Banasiak et al. (2015), Palacz et al. (2015) or Haida et al. (2016a). Therefore, to illustrate the changes in the ejector shape after optimisation, i.e., the ratio between the base and optimal geometrical, the following parameter is presented (Eq. (5)).

$$\varphi = \frac{y_{OPT}}{y_{BASE}} \tag{5}$$

The $\varphi$ for all of the considered ejectors is presented in Table 3. As can be seen, the mixer length increased for all of the ejectors, whereas the mixer diameter remained essentially the same as that of the base design. The changes of that section of the ejector are consistent with the changes presented by Palacz et al. (2016). However, the dimensions describing the nozzles geometry changed significantly. These findings show how different the influence of specific parts on the $\eta_{EJ}$ is. The relation between the diameter of the constant cross-section part of the mixer and the motive nozzle outlet diameter influence the ejector performance notably. However, the variation of the modification of $\gamma_{CON}$ did not affect the ejector performance significantly. As can be seen, the average

Table 3 – Difference between the optimised and reference ejector geometry

| Dimension | EJ1 | EJ2 | EJ3 | EJ4 |
|-----------|-----|-----|-----|-----|
| $L_{MIX}$ | 1.36 | 1.29 | 1.35 | 1.51 |
| $D_{MIX}$ | 0.96 | 0.95 | 0.96 | 0.97 |
| $L_{MCH}$ | 1.29 | 1.36 | 1.57 | 1.38 |
| $\gamma_{DIV}$ | 1.47 | 1.45 | 1.34 | 1.74 |
| $\gamma_{CON}$ | 1.02 | 0.98 | 0.57 | 1.23 |
| $D_{MN}$ | 1.09 | 1.07 | 1.09 | 1.12 |

increase in the mixer length was 37% for all ejectors. A similar trend was noted for the pre-mixing chamber length. The average increase of the parameters was 40%. The deviation of $\gamma_{CON}$ oscillated around 2% for ejectors 1 and 2. However, the changes of that dimension for EJ3 and EJ4 were much more substantial. The variation in the parameters that describe the motive nozzle shape showed that a longer diverging motive nozzle with a slightly larger outlet diameter makes the efficiency increase possible.

All of the geometry changes affected the flow field of the refrigerant inside the ejectors. The differences between the reference and the optimum flow fields were assessed for OR 1 presented in Table 1. This operating regime was used to perform the analysis presented in this section. The extended motive nozzle diverging part and longer pre-mixing chamber have a notable impact on the expansion profile. The comparison of the pressure field from the reference design and the optimised design is presented in Fig. 5. For the optimised design, the lowest pressure region occurred at the end of the motive nozzle but still inside its diverging part, whereas for the base design, it occurred inside the pre-mixing chamber. Moreover, by analysing the pressure and velocity profiles, the pressure drop inside the motive nozzle was found to be much smoother for the optimised geometry. It can be seen that the pressure at the motive nozzle outlet is lower by approximately 5 bar for the optimised device, which is particularly noticeable for the EJ1 geometry.

The increase in the distance between the motive nozzle outlet and the constant cross-section part of the mixer (longer pre-mixing chamber) affects momentum transfer inside the pre-mixing chamber. The change in the motive nozzle position relative to the mixer generates additional space for the entrained fluid when denser primary fluid flows along the axis of the ejector. Moreover, because of the low suction nozzle mass flow rate, secondary fluid tends to circulate. Fluid circulates inside the base ejector design. A similar behaviour was observed for all of the ejectors. The flow paths illustrating the phenomena for EJ1 and EJ2 are presented in Fig. 6. The circulation near the walls affects the momentum transfer between the primary and secondary fluid and increases the turbulence intensity inside the mixer. A comparison of the turbulence intensity inside the reference geometry and the optimised EJ1 and EJ2 is presented in Fig. 7. It can be observed that the turbulence in the base ejector designs is more intensive, particularly near the walls. Moreover, the primary fluid core is shorter inside the optimised devices. The reason for this behaviour is because of the better mixing performance of the primary and secondary fluids. Hence, the momentum transfer and the phase change of the primary fluid improved for the optimised ejector.

Another result of the improved mixing inside the ejector is the higher velocity inside the mixer of the device.
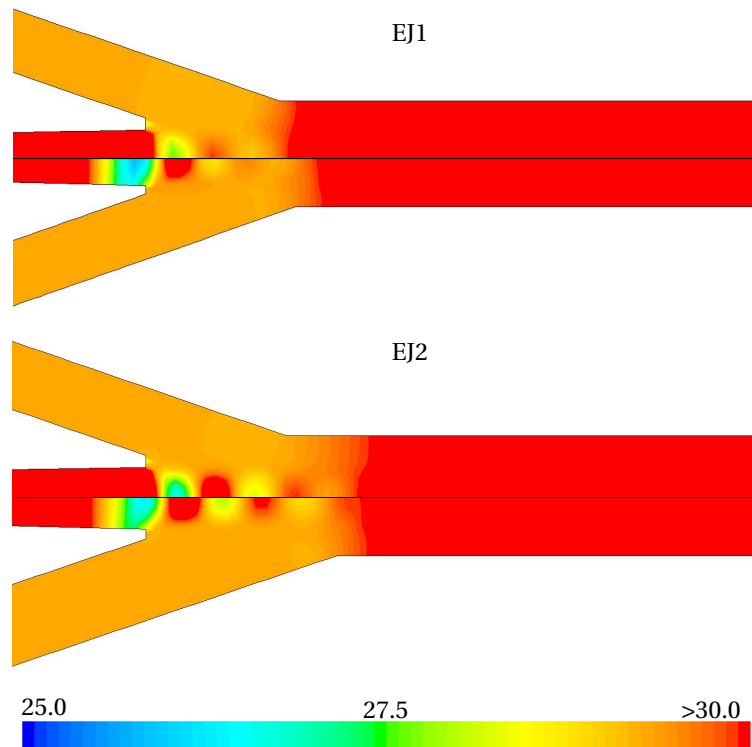
Fig. 5 – Absolute pressure field in bar: the base (top half) and optimal (bottom half) mixer of EJ1 and EJ2
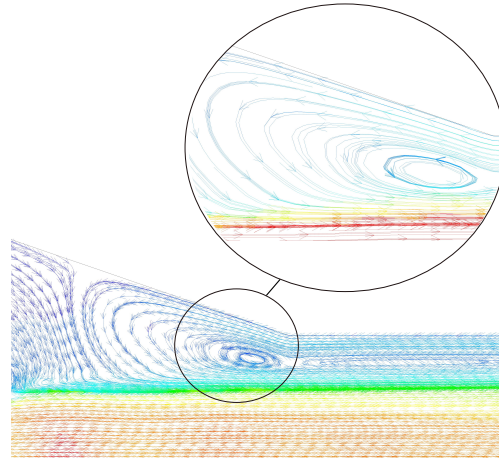


Fig. 6 – The circulation of the $CO_2$ inside the base EJ2 pre-mixing chamber

The pressure and velocity profiles for EJ1 and EJ2 are presented in Fig. 8. Similar to the previous figures, the paths presented in Fig. 8 were generated for OR 1 from Table 1. The effects of the optimisation on the flow profiles are particularly noticeable in the figure. The minimal pressure inside the mixer was approximately the same for the optimal and base ejectors. However, inside the optimal ejector, expansion of the fluid occurred inside the motive nozzle only, whereas in the baseline design, the pressure still decreased inside the pre-mixing chamber. Moreover, it can be seen that the velocity of the fluid at the mixer inlet was the same before and after the optimisation procedure. However, due to the improved momentum transfer inside the constant cross-section of the mixer, the
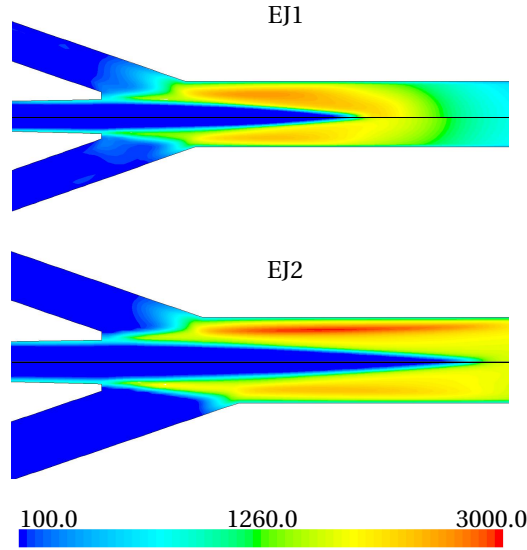
Fig. 7 – Turbulent intensity in % inside the baseline (top) and optimal (bottom) mixer of EJ1 and EJ2

velocity of the fluid is higher at the mixer centre and the mixer outlet of the optimal ejector. The velocity of the refrigerant is approximately $10\,\mathrm{m\cdot s^{-1}}$ higher for the optimised geometries at the mixer outlet section. On the other hand, the pressure profile inside the mixer was the same for the baseline and optimal design. Hence, the modifications of the ejector did not affect the pressure increase inside the mixer. These trends were observed for all the considered ejectors. Moreover, because of the improved momentum transfer, the velocity field for the optimised device is more uniform comparing to the base design. The uniformity was defined as the ratio between the average velocity magnitude to maximum velocity magnitude in a considered section (Eq. (6)).

$$u_{UNI} = \frac{|u_{AVG}|}{|u_{MAX}|} \tag{6}$$

Within this definition, if $u_{UNI}$ is closer to 1, then the velocity is more uniform in the considered section. The $u_{UNI}$ was assessed for OR 1 in Table 1 for the mixer inlet, mixer centre and mixer outlet for the reference design and optimal design. The results of the analysis are presented in Table 4. As can be seen in the Table, the $u_{UNI}$ at the mixer outlet was close to 1 for EJ1 and EJ2, whereas that for EJ3 and EJ4 was far from unity. The increase in the velocity uniformity at the mixer outlet was particularly noticeable for EJ3 and EJ4. The $u_{UNI}$ at the mixer centre significantly improved for all of the ejectors. The greater improvement for that section was for EJ4. The low values of $u_{UNI}$ at the mixer inlet were a result of the dominating high velocity of the expanding and accelerating primary fluid inside the divergence part of the motive nozzle. However, the improved uniformity inside the mixer centre was the result of the improved mixing of the motive and suction fluid. Consequently, the improved mixing process affected the relatively high uniformity inside that section. Moreover, comparing $u_{UNI}$ and the turbulence intensity presented in Fig. 7 it can be seen that the improved momentum transfer reduced the turbulence intensity inside the mixer. Analysing the $u_{UNI}$ improvements presented in Table 4 and $\eta_{EJ}$ in Table 5, it can be seen that the velocity uniformity was not necessarily results in an efficiency increase. Nevertheless, the velocity uniformity is an extremely important factor for the mixing process.

### 4.1. Efficiency improvements

First, the efficiency of the ejectors was evaluated for the base design. The $\eta_{EJ}$ and $\chi$ were calculated for the ORs presented in Table 1 and then averaged as in the OF$_4$. The average efficiency evaluated by the aforementioned method was approximately 25%, and the average mass entrainment ratio was 0.24 for all ejectors. These values were assumed as the reference ejector performance indicators. Finally, after the optimisation procedure, the reference values were compared to the ejector performance of the optimal design. The results of the comparison are
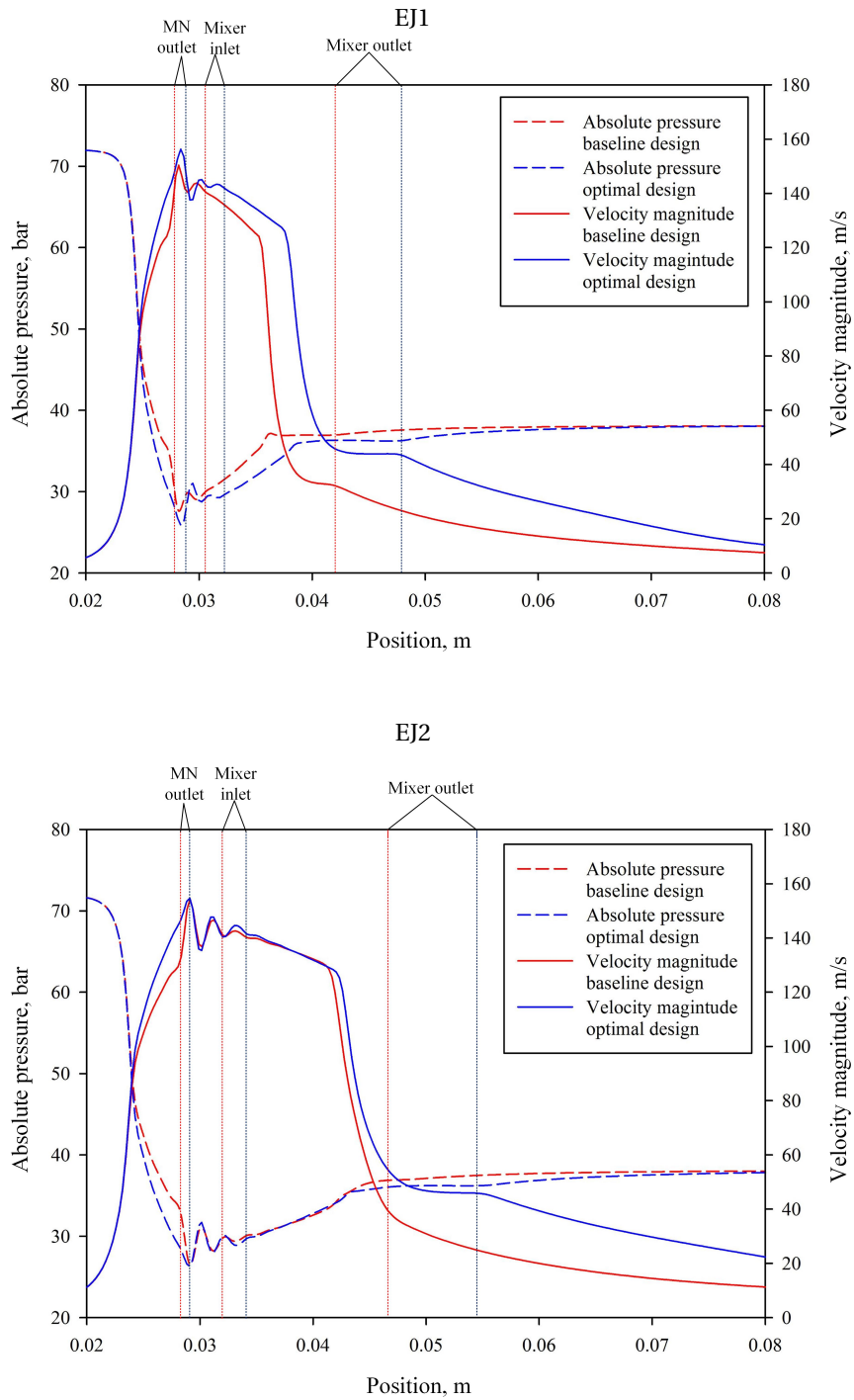
11

Fig. 8 – Pressure and velocity profiles of the baseline (red lines) and optimum (blue lines) for the EJ1 and EJ2 geometries

presented in Table 5. Moreover, the improvement of the ejector efficiency are highlighted in the Table. The average efficiency improved by 5% compared with that of the base design. As can be seen, the highest efficiency improvement was for EJ2, and the lowest increase was for EJ4. Consequently, the χ of the optimum ejector shape increased

Table 4 – $u_{UNI}$ before and after optimisation

| Cross-section | EJ1 | | EJ2 | | EJ3 | | EJ4 | |
|---|---|---|---|---|---|---|---|---|
| | BASE | OPT | BASE | OPT | BASE | OPT | BASE | OPT |
| Mixer inlet | 0.36 | 0.39 | 0.59 | 0.61 | 0.37 | 0.39 | 0.37 | 0.39 |
| Mixer centre | 0.39 | 0.72 | 0.53 | 0.77 | 0.36 | 0.66 | 0.36 | 0.72 |
| Mixer outlet | 0.97 | 0.98 | 0.96 | 0.99 | 0.75 | 0.98 | 0.64 | 0.99 |

for all ejectors. Taking into account the high reference $\eta_{EJ}$, the average efficiency increase of 5% is considered significant. Moreover, the obtained $\eta_{EJ}$ increase was notably higher than that for the mixer shape optimisation (see Palacz et al. (2016)).

However, to ensure that the optimal design is efficient for different ORs than that used in the objective function, the efficiency of the base ejector shape and the optimum ejector shape was assessed for other 10 ORs. Similar to the ORs used in the objective function, the operating regimes used for the verification procedure were captured during the experimental investigation of the considered ejectors. The range of the motive nozzle test conditions varied from 74 bar to 98 bar for pressure and from 26°C to 38°C for temperature. Moreover, five of the selected suction side operating regimes were typical food storage conditions, whereas the other five were more typical for air conditioning purposes. The temperature range for the AC conditions was between 16°C to 23 °C, and for the food storage condition, the suction nozzle temperatures ranged from 0 °C to 10 °C. Therefore, the efficiency of the designed ejectors was assessed for slightly different refrigeration system configurations.

The improvement of $\eta_{EJ}$ for the tested ORs is presented in Fig. 9. As can be seen, the average increase for all considered ejectors was 5%. This value is consistent with the efficiency improvement for the ORs used in the objective function. Consequently, the efficiency increase was the most significant for EJ2. The average EJ2 $\eta_{EJ}$ for the test points before optimisation was 30.32% and after optimisation, was 36.03%. It is also worth mentioning that the noted improvements were at a similar level for the AC conditions and the food storage conditions. Considering that the efficiency increased for both the OF and all tested ORs, there was no need to include more ORs into the OF. In consequence, the optimisation time was lower than that of Palacz et al. (2016).

## 5. Conclusions

The developed optimisation procedure can be successfully applied as a design tool for four $CO_2$ ejectors. These ejectors were originally designed for a supermarket refrigeration system. The optimisation of the shape of the ejector nozzles along with the mixer resulted in a significant efficiency increase of approximately 6%. Moreover, a verification procedure was introduced to assess the efficiency improvements for 10 additional test ORs. The verification procedure results showed an average $\eta_{EJ}$ increase of 5.2% for all optimised ejectors.

Six geometrical parameters were considered within the optimisation procedure. Three of them describe the mixer geometry ($D_{MIX}$, $L_{MIX}$ and $L_{MCH}$), and the remaining three parameters describe the ejector nozzles ($D_{MN}$, $\gamma_{DIV}$ and $\gamma_{CON}$). The mixer was extended for all four ejectors; however, the mixer diameter remained approximately the same as that of the base ejector shape. Moreover, the motive nozzle diverging angle increased after optimisation as well as the motive nozzle outlet diameter. An analysis of the results showed that the suction nozzle shape had a less significant influence on the ejector performance than the motive nozzle geometry and the mixer geometry.

Table 5 – Mass entrainment ratio and ejector efficiency for the baseline and the optimised ejector shape

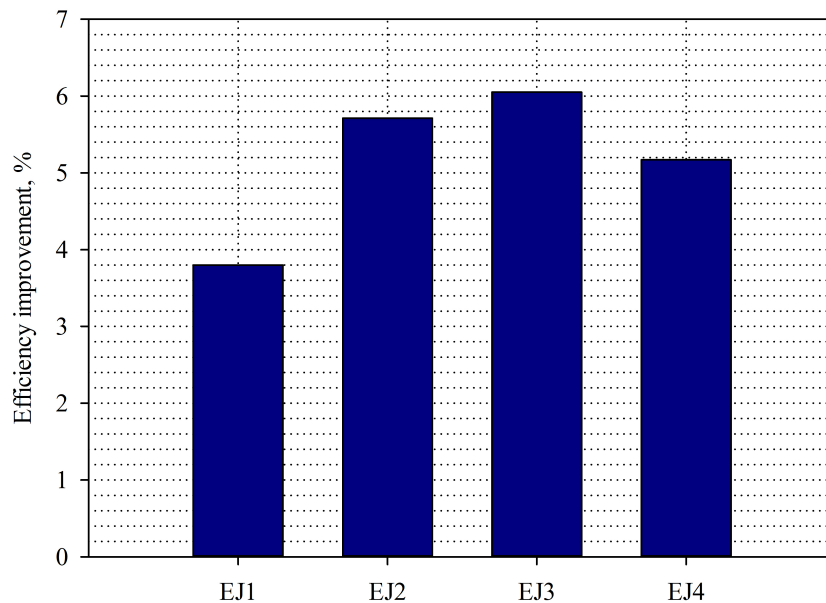| | EJ1 | | EJ2 | | EJ3 | | EJ4 | |
|---|---|---|---|---|---|---|---|---|
| | BASE | OPT | BASE | OPT | BASE | OPT | BASE | OPT |
| $\chi$, - | 0.23 | 0.27 | 0.23 | 0.28 | 0.24 | 0.28 | 0.25 | 0.29 |
| $\eta_{EJ}$, % | 24.37 | 30.00 | 24.85 | 31.20 | 25.42 | 30.87 | 26.89 | 31.44 |
| $\Delta\eta_{EJ}$, % | **5.64** | | **6.36** | | **5.45** | | **4.55** | |

Fig. 9 – Efficiency improvements for the tested ORs

The $CO_2$ flow fields after optimisation changed notably. The expansion of the primary fluid occurred much more smoothly compared with that of the base design. Moreover, a significant difference in the velocity and turbulence intensity inside the mixer was observed. The turbulence was less intense inside the optimised device, particularly near the mixer walls compared with that of the reference geometry, which affected the mixing performance and momentum transfer inside this section of the device. As a result, the difference between the average velocity and maximal velocity inside the mixer was smaller for the optimised ejector.

The presented methodology along with the robust, efficient computational tool can be effectively used for ejector design. In addition, the optimisation results can be obtained within an acceptable time. Moreover, taking into account the flexibility and accuracy of the presented computational tool (*ejectorPL*), the optimisation procedure can be used for the shape optimisation of ejectors for various working fluids.

## Acknowledgements

## References

Banasiak, K., Hafner, A., 2011. 1D computational model of a two-phase R744 ejector for expansion work recovery. Int. J. Therm. Sci. 50, 2235 – 2247.

Banasiak, K., Hafner, A., Andresen, T., 2012. Experimental and numerical investigation of the influence of the two-phase ejector geometry on the performance of the R744 heat pump. Int. J. Refrigeration 35 (6), 1617 – 1625.

Banasiak, K., Hafner, A., Kriezi, E. E., Madsen, K. B., Birkelund, M., Fredslund, K., Olsson, R., 2015. Development and performance mapping of a multi-ejector expansion work recovery pack for R744 vapour compression units. Int. J. Refrigeration.

Banasiak, K., Palacz, M., Hafner, A., Bulinski, Z., Smolka, J., Nowak, A. J., Fic, A., 2014. A CFD-based investigation of the energy performance of two-phase R744 ejectors to recover the expansion work in refrigeration systems: An irreversibility analysis. Int. J. Refrigeration 40, 328 – 337.

Besagni, G., Mereu, R., Inzoli, F., 2016. Ejector refrigeration: A comprehensive review. Renew. Sust. Eerg. Rev. 53, 373 – 407.

Corriveau, G., Guilbault, R., Tahan, A., 2010. Genetic algorithms and finite element coupling for mechanical optimization. Adv. Eng. Softw. 41, 422 – 426.

Elbel, S., 2011. Historical and present developments of ejector refrigeration systems with emphasis on transcritical carbon dioxide air-conditioning applications. Int. J. Refrigeration 34, 1545 – 1561.

Elbel, S., Hrnjak, P., 2008. Experimental validation of a prototype ejector designed to reduce throttling losses encountered in transcritical R744 system operation. Int. J. Refrigeration 31, 411 – 422.

Elbel, S., Lawrence, N., 2016. Review of recent developments in advanced ejector technology. Int. J. Refrigeration 62, 1 – 18.

Girotto, S., 2012. Efficiency improvement in commercial refrigeration for warmer climates with $CO_2$. Proceedings from the ATMOsphere Europe 2012, 5-7.11.2012, Brussels.

Hafner, A., Försterling, S., Banasiak, K., 2014. Multi-ejector concept for R-744 supermarket refrigeration. Int. J. Refrigeration 43, 1–13.

Haida, M., Banasiak, K., Smolka, J., Hafner, A., Eikevik, T. M., 2016a. Experimental analysis of the R744 vapour compression rack equipped with the multi-ejector expansion work recovery module. Int. J. Refrigeration 64, 93 – 107.

Haida, M., Smolka, J., Palacz, M., Bodys, J., Nowak, A., Bulinski, Z., Fic, A., Banasiak, K., Hafner, A., 2016b. Numerical investigation of an r744 liquid ejector for supermarket refrigeration systems. THERM SCI 20 (4), 1259–1269.

Lawrence, N., Elbel, S., 2015. Mathematical modeling and thermodynamic investigation of the use of two-phase ejectors for work recovery and liquid recirculation in refrigeration cycles. Int. J. Refrigeration 58, 41 – 52.

Lemmon, E. W., Huber, M. L., McLinden, M. O., 2010. NIST Standard Reference Database 23: Reference Fluid Thermodynamic and Transport Properties - REFPROP. National Institute of Standards and Technology, Standard Reference Data Program, Gaithersburg, 9th Edition.

Liu, F., Groll, E. A., Li, D., 2012a. Investigation on performance of variable geometry ejectors for $CO_2$ refrigeration cycles. Energy 45, 829 – 839.

Liu, F., Groll, E. A., Li, D., 2012b. Modeling study of an ejector expansion residential $CO_2$ air conditioning system. Energ. Buildings 53, 127 – 136.

Liu, F., Li, Y., Groll, E. A., 2012c. Performance enhancement of $CO_2$ air conditioner with a controllable ejector. Int. J. Refrigeration 35, 1604 – 1616.

Lucas, C., Koehler, J., 2012. Experimental investigation of the COP improvement of a refrigeration cycle by use of an ejector. Int. J. Refrigeration 35 (6), 1595 – 1603.

Lucas, C., Rusche, H., Schroeder, A., Koehler, J., 2014. Numerical investigation of a two-phase $CO_2$ ejector. Int. J. Refrigeration 43, 154 – 166.

Munoz, A. G., Ayala-Ramirez, V., Alfaro-Ayala, J., Acosta, B. T., 2011. Optimization of the transition piece applying genetic algorithms. Appl. Therm. Eng. 31, 3214 – 3225.

Nakagawa, M., Marasigan, A., Matsukawa, T., Kurashina, A., 2011. Experimental investigation on the effect of mixing length on the performance of two-phase ejector for $CO_2$ refrigeration cycle with and without heat exchanger. Int. J. Refrigeration 34, 1604 – 1613.

Palacz, M., Smolka, J., Fic, A., Bulinski, Z., Nowak, A. J., Banasiak, K., Hafner, A., 2015. Application range of the HEM approach for $CO_2$ expansion inside two-phase ejectors for supermarket refrigeration systems. Int. J. Refrigeration 59, 251 – 258.

Palacz, M., Smolka, J., Kus, W., Fic, A., Bulinski, Z., Nowak, A. J., Banasiak, K., Hafner, A., 2016. CFD-based shape optimisation of a $CO_2$ two-phase ejector mixing section. App. Therm. Eng. 95, 62 – 69.

Sag, N. B., Ersoy, H., Hepbasli, A., Halkaci, H., 2015. Energetic and exergetic comparison of basic and ejector expander refrigeration systems operating under the same external conditions and cooling capacities. Energ. Covers. Manage. 90, 184 – 194.

Sierra-Pallares, J., del Valle, J. G., Carrascal, P. G., Ruiz, F. C., 2016. A computational study about the types of entropy generation in three different R134a ejector mixing chambers. Int. J. Refrigeration 63, 199 – 213.

Smolka, J., 2013a. CFD-based 3-D optimization of the mutual coil configuration for the effective cooling of an electrical transformer. Appl. Therm. Eng. 50, 124 – 133.

Smolka, J., 2013b. Genetic algorithm shape optimisation of a natural air circulation heating oven based on an experimentally validated 3-D CFD model. Int. J. Therm. Sci. 71, 128 – 139.

Smolka, J., Bulinski, Z., Fic, A., Nowak, A. J., Banasiak, K., Hafner, A., 2013. A computational model of a transcritical R744 ejector based on a homogeneous real fluid approach. Appl. Math. Model. 37, 1208 – 1224.

Smolka, J., Palacz, M., Bodys, J., Banasiak, K., Fic, A., Bulinski, Z., Nowak, A. J., Hafner, A., 2016. Performance comparison of fixed- and controllable-geometry ejectors in a $CO_2$ refrigeration system. Int. J Refrigeration 65, 172 – 182.

Xu, X. X., Chen, G. M., Tang, L. M., Zhu, Z. J., 2012. Experimental investigation on performance of transcritical $CO_2$ heat pump system with ejector under optimum high-side pressure. Energy 44 (1), 870 – 877.